Theoretical conformational study of poly(trans-1, 2-Di(2-thienyl) ethylene): Effects on the electronic structure and optical properties

ARTICLE *in* INTERNATIONAL JOURNAL OF QUANTUM CHEMISTRY · NOVEMBER 2006

Impact Factor: 1.43 · DOI: 10.1002/qua.21131

3 AUTHORS, INCLUDING:

Ricardo Paupitz
São Paulo State University
47 PUBLICATIONS **136** CITATIONS

SEE PROFILE

Theoretical Conformational Study of Poly(*trans*-1, 2-Di(2-Thienyl) Ethylene): Effects on the Electronic Structure and Optical Properties

NEI MARÇAL, BERNARDO LAKS, RICARDO PAUPITZ BARBOSA DOS SANTOS

Instituto de Física, Universidade Estadual de Campinas, 13083-970 Campinas, São Paulo, Brazil

Received 28 December 2005; accepted 2 May 2006
Published online 28 June 2006 in Wiley InterScience (www.interscience.wiley.com).
DOI 10.1002/qua.21131

ABSTRACT: In the present study, we investigate the monomer ethylene-bridged-bithiophene (TET) and the dimer ethylene-bridged-bithiophene $(TET)_2$ to find the more probable conformations of the oligomer and their electronic properties. Geometrical optimizations were carried out at semiempirical level using the Austin method one (AM1) and parametric method 3 (PM3). The electronic transition energies and their associated oscillator strength values are calculated for neutral oligomers. The calculations are conducted using the intermediate neglect of differential overlap Hamiltonian (INDO) in combination with a single configuration–interaction technique in order to include correlation effects. We also employ the negative factor counting (NFC) technique to obtain the electronic density of states (DOS). © 2006 Wiley Periodicals, Inc. Int J Quantum Chem 106: 2723–2730, 2006

Key words: conformational structure; semiempirical models; optical absorption spectra; electronic structure

Introduction

In the last decades, conjugated polymers have been subject of increasing interest, due to a great potential for technological applications [1] in unusual optical and electronics devices. This is because of the fundamental characteristics of conjugated polymers, which are different from those commonly found in usual inorganic semiconductor systems.

Among these characteristics, the topological defects (such as solitons, polarons and bipolarons, produced in the polymeric chain) play an important role. These structures should be responsible for the appreciable electrical conductivities that the conju-

Correspondence to: N. Marçal; e-mail: marcal@ifi.unicamp.br
Contract grant sponsors: CNPq; FAPESP; CENAPAD (Brazilian agencies); Fabiana F. Moura.

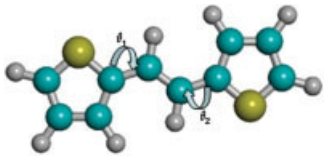

FIGURE 1. Chemical structure of the monomer ethylene-bridged-bithiophene (TET). [Color figure can be viewed in the online issue, which is available at www.interscience.wiley.com.]

gated systems have shown. Submitting these polymers to doping, either by oxidation or by reduction, may be possible to control for their electric conductivity [2], which can reach the same order of the metallic conductivity for some of them [3, 4].

Conjugated polymers are characterized by their alternation of single and double bonds among carbon atoms. This bond alternation is caused by electron–phonon interaction generating the so-called Peierls energy gap, leaving the polymeric system into a semiconducting state. In the case of a planar polymer, each atom along the backbone of the polymer contributes with a single electron in a p_z orbital. The large overlap between these orbitals p_z can originate a delocalized wave function, allowing electronic conduction when the polymer is doped. The extension of the electronic wave function is intimately linked to the planarity of the polymeric structure and the electrical conduction to the existence of unoccupied accessible states.

In the present study, we investigated the monomer ethylene-bridged-bithiophene (TET) (Fig. 1) and the dimer ethylene-bridged-bithiophene $(TET)_2$ (Fig. 2) to obtain the conformations of the oligomer, which are most likely to occur (i.e., those who have greater probability to occur) and their electronic properties. We are interested in verifying which polymeric structure can be generated by extrapolation the most probable conformational structure oligomeric.

To obtain a reasonable geometric structure for the polymer, with high molecular weight (usually in the solid state), we first proceeded by conducting some semiempirical calculations for the monomers and dimers as explained next.

Our first aim was to obtain the most probable geometric conformation of the monomer. To do that, it was necessary to generate a multiconformational surface plotting the heat of formation as a function of the torsion angles θ_1 and θ_2 (Fig. 1).

The most stable geometric conformation of the monomer was used to obtain the most stable conformation for the dimer, which was conducted by varying the dihedral angle θ_3 formed between the adjacent monomer (Fig. 2). The structure of the oligomer was generated by the structure repetition of the dimer. Such structure was optimized using semiempirical models (AM1 and PM3). In addition, we obtained the electronic density of states (DOS) and the band structure of the polymer.

With the resulting oligomeric structures, we were able to calculate the electronic transition energies and their associated oscillator strength values for neutral oligomers, thus the ultraviolet (UV)-vis absorption spectra was obtained. The calculations were conducted using the INDO Hamiltonian in combination with a single configuration-interaction technique to include correlation effects.

Methodology

For the calculations we supposed the molecules were in vacuum at 0 K, neglecting the interaction with the environment. The geometric optimization calculations were accomplished by using the General Atomic Molecular and Electronic Structure System (GAMESS) program [5] at AM1 [6] and PM3 [7] semiempirical levels.

To construct the multiconformational surface, the dihedral angles θ_1 and θ_2 were frozen, leaving the rest of the molecule free to optimize the geometry. For each geometric conformation, the torsion angles θ_1 and θ_2 were scanned independently in steps of 10°, considering all the possible angular arrangements up to 360° for each angle. Then, we determined the heat of formation for each one of the conformations.

In the case of the $(TET)_2$ (Fig. 2), the angle θ_3 was frozen, leaving the rest of the dimer free to optimize the geometry. The initial configuration structure was *anti-gauche* and we considered only the angle θ_3

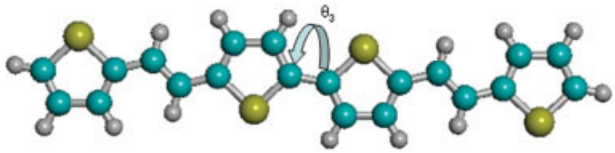

FIGURE 2. Scheme of the dimer ethylene-bridged-bithiophene $(TET)_2$, with the dihedral angle (θ_3), formed between adjacent monomer, assuming, in this case, the value 0°. [Color figure can be viewed in the online issue, which is available at www.interscience.wiley.com.]

varying with a step of 10° from 0° (planar *anti* conformer) to 180° (planar *syn* conformer). Figure 2 shows the *anti* conformer which corresponds to the most stable conformation.

To determine the percentage of each stable geometric conformation of the monomers at room temperature, we proceeded as follows. We consider that the effect of temperature on the occurrence of a particular conformer is such that the probability of a specific configuration to occur follows a Maxwell–Boltzmann distribution [8], given by

$$\text{probability} = \frac{\sum_i e^{-\frac{E_i}{kT}}}{Z},$$

where E_i is the energy calculated for each conformation defined by θ_1 and θ_2, k is Boltzmann's constant, T is the absolute room temperature (300 K), and Z is the partition function.

The electronic transition energies and their associated oscillator strength values were calculated based on the highest probability conformations. The calculations were performed by using the INDO method as parameterized by Ridley et al. [9] in combination with the single configuration interaction (SCI) technique to consider the correlation effects. This approach has been widely used to calculate optical properties of the oligomers.

In each case, the SCI included the nearest 10 occupied and unoccupied orbitals to the highest occupied molecular orbital (HOMO) and the lowest unoccupied molecular orbital (LUMO). For the neutral systems (closed shell), this choice implies 101 configurations, since the number of configuration–interaction (CI) wave functions was large enough to describe the lowest energy excited states of these systems. ZINDO/S-CI calculations with more configurations were carried out, but only discrete modifications in the UV-vis spectra were found.

The DOS of long PTE chains (≤400 rings) was obtained using the NFC technique [10]. The NFC technique allows a fast DOS calculation, avoiding the direct diagonalization of Hamiltonian matrix. The NFC technique was also originally proposed by Dean [10] for the study of vibrational spectra of linear chains and later extended [11] to the study of electronic structure. We have used the NFC technique coupled to a tight-binding (extended Hückel) Hamiltonian. The use of simple extended Hückel parameterization implies in the assumption of σ–π separability. We have used this based on the fact that the dihedral angle in the polymer is small and that the electronic structure results do not strongly depend on it.

Results

A multiconformational surface of the (TET) monomer calculated using the semiempirical PM3 Hamiltonian model is shown in Figure 3(a). This surface was obtained by having the heat of formation as a function of the change on dihedral angles θ_1 and θ_2, according to Figure 1. We obtained the heat of formation as a function of different geometric configurations. In Figure 3(b) there is a projection of multiconformational surface on θ_1, θ_2 plane. It should be noted that the minimum value of energy found in Figure 3(a) corresponds to 78.3668 kcal/mol and the torsional barrier is ~2.5 kcal/mol in height.

The multiconformational surface calculated using the AM1 model is shown in Figure 4(a) and 4(b). The minimum energy value found in this figure corresponds to 68.9966 kcal/mol and the torsional barrier is near 2.0 kcal/mol in height. In Figure 4(a), the surface is very similar to that shown in Figure 3(a), where the same methodology but different semiempirical models were used.

It was observed for both, PM3 (Fig. 3) and AM1 (Fig. 4), calculations that the minimum of the surfaces corresponded to three possible geometric conformers. These conformers are represented schematically in Figure 5.

Using the thermodynamical calculations cited previously, it was possible to determine the probability of finding each one of the more stable conformations at room temperature.

The calculations performed with the PM3 model showed that the probability of finding each geometric configuration at room temperature was 60% for configurations of Figure 5(a), 25% of that in Figure 5(b), and 15% corresponding to Figure 5(c). For the calculations performed with the semiempirical AM1 model, the results obtained for each geometric configuration at room temperature were: 40% to the corresponding configuration of Figure 5(a), 33% with respect to Figure 5(b), and 27% for configurations of Figure 5(c).

The monomer of configuration in Figure 5(b) in both models forms a helicoidal chain when the size of oligomer is increased, and this is not the ground state of the polymer. In the case of the configuration

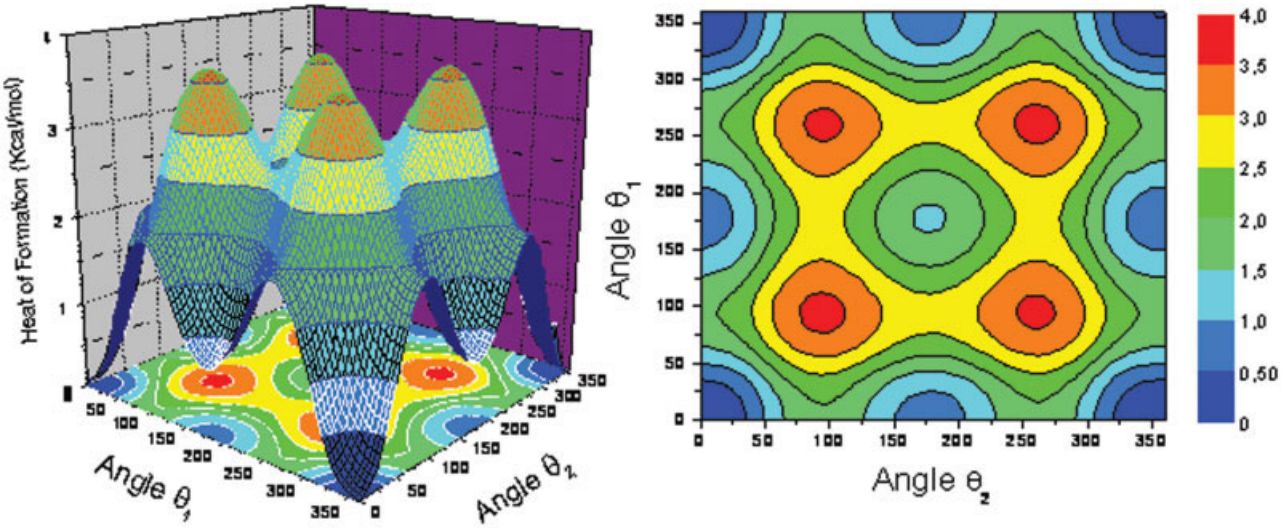

FIGURE 3. (a,b) Multiconformational surface and curves of levels of multiconformational surface the monomer (TET) respectively, calculated with the semiempirical PM3 model. The vertical axis represents the total energy difference between the most stable system and the other conformations. [Color figure can be viewed in the online issue, which is available at www.interscience.wiley.com.]

shown in Figure 5(c), the steric interactions between the sulfur atoms and the hydrogen atoms of adjacent rings, resulted in a structure with greater heat of formation. These conclusions were obtained through the calculations with oligomers composed of 1–6 monomers, in each of the following configurations, 5a, 5b, and 5c.

It is important to note that the semiempirical models used, AM1 and PM3, produced different values of bond lengths and angles in the resulting monomer. Qualitatively, the multiconformational surfaces generated by both models were similar. Table I shows the smaller heat of formation to each type (A, B, C) of isomers (Fig. 5). As you can see, these values are very close for both models used in the calculation.

Furthermore, Table I details the geometrical conformations presented schematically in Figure 5. The

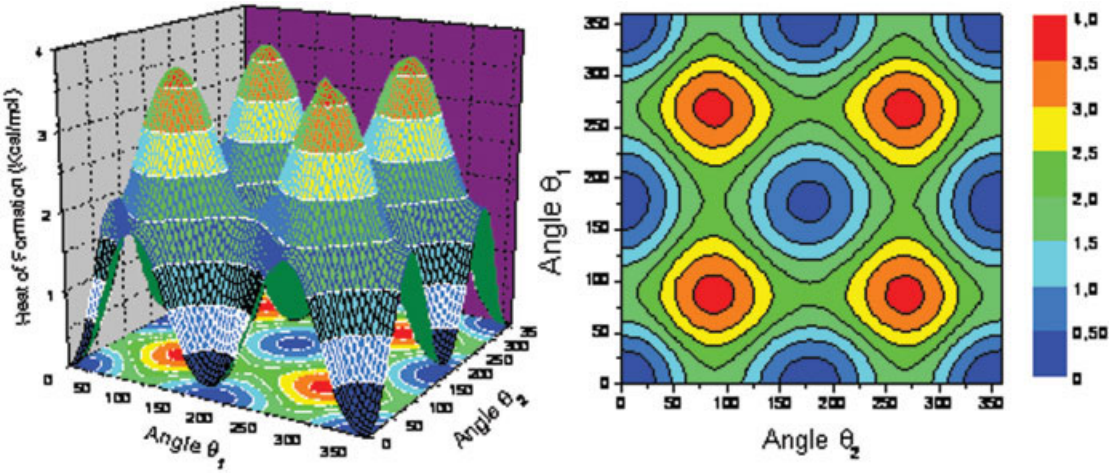

FIGURE 4. (a,b) Multiconformational surface and curves of levels of multiconformational surface the monomer (TET) respectively, calculated with the semiempirical AM1 model. The vertical axis represents the total energy difference between the most stable system and the other conformations. [Color figure can be viewed in the online issue, which is available at www.interscience.wiley.com.]

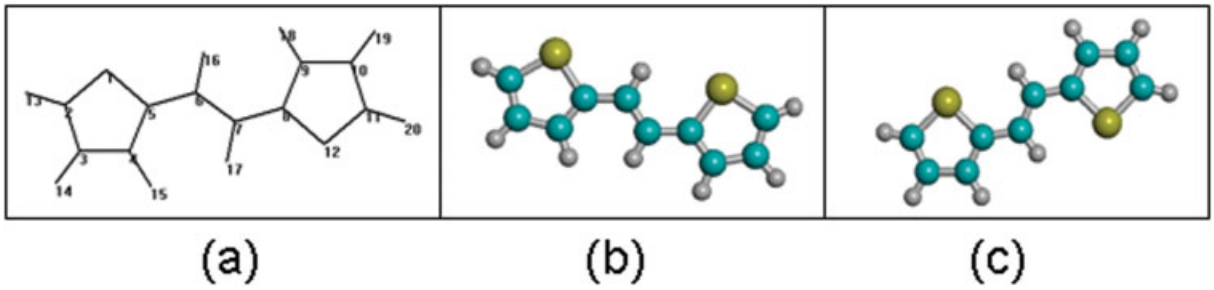

FIGURE 5. Chemical structure of TET by resultant isomers most stable. In (a) was displayed a number of scheme used to identify the atoms in TET monomer in text. [Color figure can be viewed in the online issue, which is available at www.interscience.wiley.com.]

superscript indices over the atom symbols correspond to the numeric scheme seen in Figure 5(a). We also presented bond lengths obtained with AM1 and PM3 models and with experimental data [12]. We showed also the angle between adjacent bonds where vertices atoms are indicated by an underlined number. The heats of formation for each one of the conformers are presented in last column. Finally, the dihedral angles are indicated by four numbers following the numeration scheme used in Figure 5(a) in the last column.

TABLE I

Equilibrium geometry [bond length (Å), angle (°), dihedral angle (°)] for monomers with higher probabilities (Fig. 5) and their heats of formation (kcal/mol).

Type A	$^{1}S—^{2}C$ (Å)	$^{2}C=^{3}C$ (Å)	$^{3}C—^{4}C$ (Å)	$^{4}C=^{5}C$ (Å)	$^{1}S—^{5}C$ (Å)	$^{5}C—^{6}C$ (Å)	$^{6}C=^{7}C$ (Å)	Heat of formation (kcal/mol)	
PM3	1.7210	1.3665	1.4316	1.3753	1.7454	1.4428	1.3446	78.3668	
AM1	1.6659	1.3787	1.4271	1.3865	1.6890	1.4327	1.3475	68.9966	
Expt.[a]	1.701	1.351	1.44	1.40	1.701	1.457	1.309	#####	
	Angle 1$\underline{2}$3	Angle 2$\underline{3}$4	Angle 3$\underline{4}$5	Angle 4$\underline{5}$1	Angle 5$\underline{1}$2	Angle 4$\underline{5}$6	Angle 5$\underline{6}$7	Angle 4567	Angle 5678
PM3	112,41	112,414	112,615	111,135	91,4259	127,109	123,129	0	180
AM1	111,813	111,682	111,901	110,608	93,9955	128,138	124,264	0	180

Type B	$^{1}S—^{2}C$ (Å)	$^{2}C=^{3}C$ (Å)	$^{3}C—^{4}C$ (Å)	$^{4}C=^{5}C$ (Å)	$^{1}S—^{5}C$ (Å)	$^{5}C—^{6}C$ (Å)	$^{6}C=^{7}C$ (Å)	Heat of formation (kcal/mol)	
PM3	1.7214	1.3663	1.4312	1.3762	1.7468	1.4445	1.3437	78.8099	
AM1	1.6656	1.3789	1.4262	1.3879	1.6892	1.4335	1.3471	69.3307	
	Angle 1$\underline{2}$3	Angle 2$\underline{3}$4	Angle 3$\underline{4}$5	Angle 4$\underline{5}$1	Angle 5$\underline{1}$2	Angle 4$\underline{5}$6	Angle 5$\underline{6}$7	Angle 4567	Angle 5678
PM3	112,521	112,32	112,712	111,055	91,3913	123,333	123,726	180	180
AM1	111,899	111,614	111,963	110,547	93,9769	124,732	124,215	180	180

Type C	$^{1}S—^{2}C$ (Å)	$^{2}C=^{3}C$ (Å)	$^{3}C—^{4}C$ (Å)	$^{4}C=^{5}C$ (Å)	$^{1}S—^{5}C$ (Å)	$^{5}C—^{6}C$ (Å)	$^{6}C=^{7}C$ (Å)	Heat of formation (kcal/mol)	
PM3	1.7207	1.3666	1.4314	1.3754	1.7451	1.4428	1.3442	79.1132	
AM1	1.6663	1.3785	1.4272	1.3864	1.6891	1.4322	1.3474	69.1592	
	Angle 1$\underline{2}$3	Angle 2$\underline{3}$4	Angle 3$\underline{4}$5	Angle 4$\underline{5}$1	Angle 5$\underline{1}$2	Angle 4$\underline{5}$6	Angle 5$\underline{6}$7	Angle 4567	Angle 5678
PM3	112,516	112,335	112,713	111,057	91,3799	123,332	123,684	180	180
AM1	111,902	111,613	111,952	110,561	93,972	124,764	124,312	180	180

[a] Experimental geometry from Ref. [12].

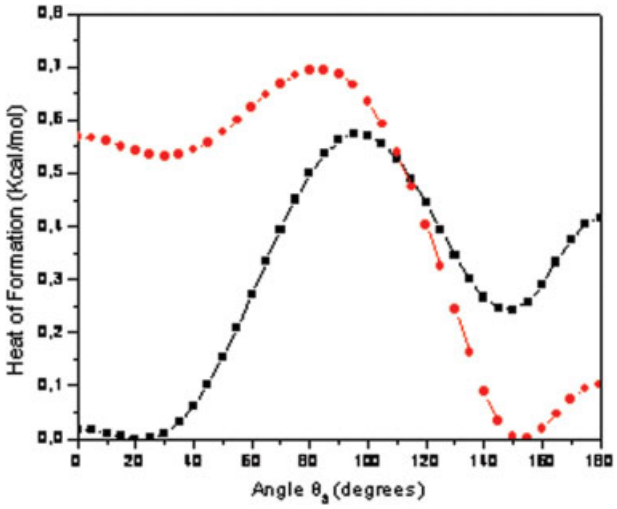

FIGURE 6. Energy difference between the most stable system and the other conformations as a function of the torsion angle θ_3. Both were calculated with semiempirical PM3 (circle) and AM1 (square) models. In these calculations, starting angle was $\theta_3 = 0°$ for an anti-planar configuration. [Color figure can be viewed in the online issue, which is available at www.interscience.wiley.com.]

To obtain the most stable dimer $(TET)_2$, we calculated the heat of formation as a function of the variation of angle θ_3 from 0 to 180° (Fig. 6). The monomer chosen to build the dimer, was the one for which we found the highest probability in the thermodynamic calculation, which corresponds to the monomeric configuration of the Figure 5(a).

The result generated by the calculation with the model PM3 presents a minimum near 155°, although the result obtained by the AM1 model displays a minimum about 20°. In our calculation with bithiophene, the PM3 model generated a configuration *syn* to minimal energy, while the AM1 model generated results with a configuration *anti* with a angle of 28° between the rings the bithiophene. In the case of $(TET)_2$, we are varying the angle (θ_3) between adjacent thiophene rings, and it is natural to expect the reproduction in part of the effects verified on bithiophene. It is reported in the literature that polythiophene has an *anti* planar conformation [13–15]. Therefore, by analogy with the polythiophene, we expect that the poly-*trans*-(1-2di(thienyl)ethylene) *trans*-PTE presents a configuration *anti* as well. Therefore, the PTE is a repetition of the geometric structure from Figure 2. Furthermore, it is known from the literature that Polythiophene presents a great planarity due to the packing effect of its chains. We believe that the same effect should occur in PTE, since its oligomer structure presents a greater planarity than the thiophene oligomer, due to the separation between the rings by ethylene groups.

Since we were interested in electronic transition energies. The calculations made for oligomers with sizes from 2 up to 6 oligomers, using INDO/SCI showed that the lower energy absorption peak corresponds essentially to an electronic transition between HOMO ($|H\rangle$) and LUMO ($|L\rangle$). We also observed that as long as we increased the size of oligomers, the absorption peak suffered a red shift. The absorption peaks showed in Table II correspond to higher oscillator strengths, although the calculation showed the existence of a second absorption of least importance [16]. The first peak refers to a polymer gap localized at ~2.0 eV, while the second one refers to an interband transition at ~2.6 eV. Both peaks were experimentally obtained [17, 18]. The more we increased the chain size, the more we observed the convergence of calculated results toward experimentally obtained values [17, 18].

Table II presents a description (in terms of configuration-interaction expansion) of absorption peaks in several oligomers. As with oligothiophenes [19], it was observed the existence of a quasi electron-hole symmetry in the oligo(*trans*-PTE) highlighted by the nature of configurations associated to greatest CI expansion coefficients. Besides, we realized that the linear combination of atomic orbital (LCAO) coefficients on the carbon atoms that originate bonding-antibonding patterns are only possible due to the symmetry group held by the system of excited state.

Figure 7 displays both models AM1 and PM3 values of absorption (Table II) as a function the size of the oligomer, ranging from 2 up to 6 monomers. To obtain the gap to poly-*trans*(1-2di(thienyl)ethylene) *trans*-PTE, we performed a linear fit of the data and we noted those values of extrapolated transitions are near known experimental results to the gap [17, 18]. The values obtained to gap were 2.06 eV to PM3 and 1.89 eV to AM1 models.

Figure 8 (right side) displays the structure of bands of the π orbitals of a long PTE chain, which was obtained by using a tight-binding Hamiltonian. The left side shows the density of electronic states DOS for the PTE neutral, which was obtained by using the NFC technique. This calculation was accomplished by taking into consideration the repetition of geometry obtained by the central unit (one dimer) oligomer. The hopping between atoms was

TABLE II

ZINDO/S transition energies, oscillator strengths, and main CI expansion coefficients of the lowest-energy absorption peak in the neutral *trans*-PTE oligomers.

PM3 model			
No. of repeat units	Transition energies (eV)	Oscillator strengths	Main CI expansion coefficients of the excited states
2	2,629	2,12	$0{,}88\|H \rightarrow L\rangle$
3	2,385	3,03	$0{,}77\|H \rightarrow L\rangle + 0{,}15\|H - 1 \rightarrow L + 1\rangle$
4	2,276	3,93	$0{,}65\|H \rightarrow L\rangle + 0{,}19\|H - 1 \rightarrow L + 1\rangle$
5	2,220	4,85	$0{,}58\|H \rightarrow L\rangle + 0{,}20\|H - 1 \rightarrow L + 1\rangle$
6	2,191	5,76	$0{,}50\|H \rightarrow L\rangle + 0{,}21\|H - 1 \rightarrow L + 1\rangle + 0{,}11\|H - 2 \rightarrow L + 2\rangle$
AM1 model			
No. of repeat units	Transition energies (eV)	Oscillator strengths	Main CI expansion coefficients of the excited states
2	2,505	2,18	$0{,}88\|H \rightarrow L\rangle$
3	2,240	3,09	$0{,}79\|H \rightarrow L\rangle + 0{,}14\|H - 1 \rightarrow L + 1\rangle$
4	2,122	3,99	$0{,}69\|H \rightarrow L\rangle + 0{,}17\|H - 1 \rightarrow L + 1\rangle$
5	2,059	4,91	$0{,}60\|H \rightarrow L\rangle + 0{,}20\|H - 1 \rightarrow L + 1\rangle$
6	2,027	5,84	$0{,}52\|H \rightarrow L\rangle + 0{,}21\|H - 1 \rightarrow L + 1\rangle + 0{,}10\|H - 2 \rightarrow L + 2\rangle$

H, highest occupied molecular orbital (HOMO); L, lowest unoccupied molecular orbital (LUMO).

obtained using the geometry of a central unit oligomeric calculated by the semiempirical model (AM1). While the parameter K of Clementi's parameterization [20] was optimized to describe the band gap of 2.1 eV of PT obtained experimentally [21]. $K = 2.01$ was the parameter value used.

In Figure 8, the top of the valence band (HOMO) has a value of −10.02 eV and the bottom of con-

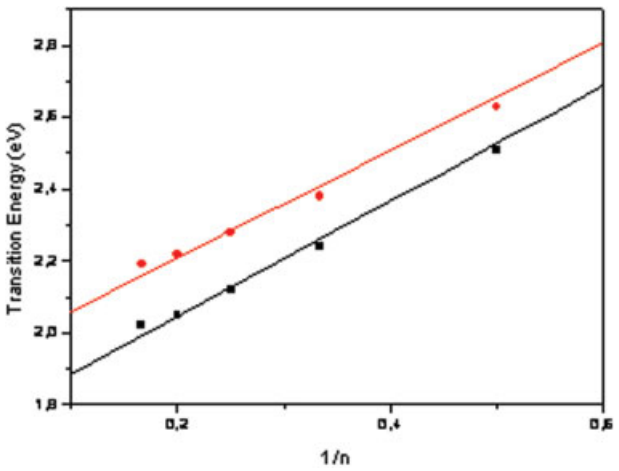

FIGURE 7. Evolution of the INDO/SCI-PM3, AM1 (circle and squares respectively) calculated transition energies of neutral oligo(*trans*-PTE) as a function of the inverse of the number of oligomers (1/*n*). [Color figure can be viewed in the online issue, which is available at www.interscience.wiley.com.]

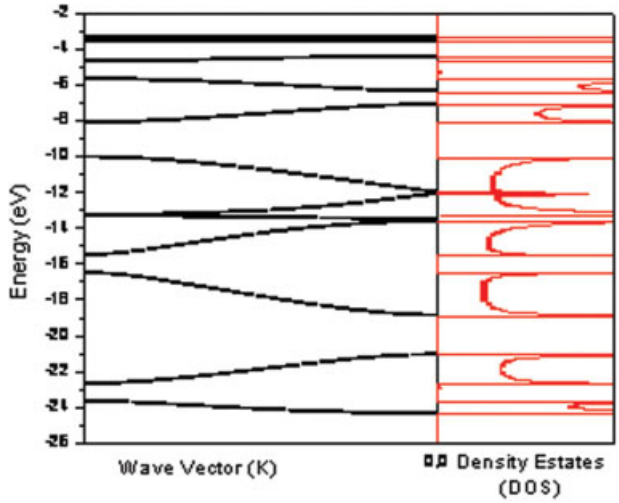

FIGURE 8. At the left side PTE, band structure of the orbitals π. At the right side, the DOS of PTE polymer obtained through NFC technique. [Color figure can be viewed in the online issue, which is available at www.interscience.wiley.com.]

duction band (LUMO) corresponds to −8.19 eV, both calculated using the extended Hückel model generating a gap of 1.83 eV.

The experimental result to the gap is equal to 1.9 eV [17, 18], which is similar to the obtained theoretically a value of 1.83 eV.

Conclusion

The most likely geometric conformation of the monomer TET was shown by both AM1 and PM3 semiempirical calculations. Our results obtained with the semiempirical PM3 model for $(TET)_2$ presented the same effects of the PT between the thiophene rings. Our calculations showed that PTE presents a chain that is not planar, due to interaction between the thienyl rings. This interaction increases in case of PT, producing a greater torsion between the thienyl rings.

When there is an interaction among neighboring chains (PTE), these chains tend to a planar conformation due to packing effects [22]. In addition, we observed that polymeric configuration present smaller dihedral angles between the rings than those found in the PT. The presence of the bridge between the rings increases the planarity of chain.

We noted for both (AM1 and PM3) semiempirical calculations, that the more we increased the size of the oligomeric chain, the UV-vis absorption spectra assumed lower energy values, and the oscillator strength increases for the first absorption, while for the second absorption, the oscillator strength decreases.

The band structure and the DOS of the polymer indicate that the *trans*-(PTE) have a band gap smaller than the PT and bigger than the polyacetylene (PA) band gap. One explication for this effect is the fact that the *trans*-(PTE) has a major planarity caused by the ethylene-bridged structure. In other words, because the copolymer is a mixture between the two polymers, it is expected that the PTE gap has an intermediate value between the PT and the PA gap.

References

1. Street, G. B. In Handbook of Conducting Polymers; Vol 1; Skotheim, T. A., Ed.; Marcel Dekker: New York, 1986.
2. Marçal, N.; Laks, B. Int J Quantum Chem 2003, 95, 230.
3. Tsukamoto, J. Adv Phys 1992, 41, 509.
4. Satoh, M.; Imanishi, K.; Yasuda, Y.; Tsushima, R.; Yamasaki, H.; Aoki, S. Synth Met 1989, 30, 33.
5. Schimidt, M. W.; Baldridge, K.; Boatz, J. A.; Elbert,. S. T.; Gordon, M. S.; Jensen, J. H.; Koseki, S.; Matsunaga, N.; Nguyen, K. A., Su, S. J.; Windus, T. L.; Dupuis, M.; Montgomery, J. A. J Comput Chem 1993, 14, 1347.
6. Dewar, M. J. S.; Zoebisch, E. G.; Healy, E. F.; Stewart, J. J. P. J Am Chem Soc 1985, 107, 3902.
7. Stewart, J. J. P. J Comput Chem 1989, 10, 209.
8. Richards, W.G. Quantum Pharmacology; Butter & Tanner Ltd: Great Britain, 1977.
9. Ridley, J.; Zener, M. Theor Chim Acta 1976, 42, 223.
10. (a) Dean, P. Phys Soc (London) 1959, 73, 413; (b) Ladik, J.; Seel, M.; Otto, P.; Bakhshi, A. K. Chem Phys 1986, 108, 2003.
11. Seel, M. Chem Phys 1979, 43, 103.
12. Ruban, G.; Zobel, D. Acta Crystallogr B 1975, 31, 2632.
13. Cui, C. X.; Kertesz, M. Phys Rev B1989, 40, 9661.
14. Almennigen, A.; Bastiansen, O.; Svendsas, P. Acta Chem Scand 1958, 12, 1671.
15. Helio, A. D.; Helio, F. S.; Willian, R. R.; Wagner, B. A. J Chem Phys 2000, 113, 4206.
16. Marçal, N.; Laks, B. Int J Quantum Chem 2005, 103, 617.
17. Onoda, M.; Iwasa, T.; Kawai, T.; Yoshino, K. Synth Met 1993, 55, 1647.
18. Onoda, M.; Iwasa, T.; Kawai, T.; Yoshino, K. Appl Phys 1991, 24, 2076.
19. Cornil, J.; Beljonne, D.; Bredas, J. L. J Chem Phys 1995, 103, 842.
20. Clementi, E.; Raimondi, D. L. J Chem Phys, 1963, 39, 1397.
21. Onoda, M; Iwasa, T.; Kawai, T.; Yoshino, K. J Phys D: Appl Phys 1991, 42, 2076.
22. Eckhardt, H.; Shacklette, L. W.; Jen, K. Y.; Elsenbaumer, R. L. J Chem Phys 1989, 91, 1303.